Diabetes, Metabolic Syndrome and Obesity

Dovepress
Taylor & Francis Group

Open Access Full Text Article

ORIGINAL RESEARCH

Combining Network Pharmacological Analysis and Animal Experiments to Explore the Pharmacological Mechanism of Zhangyanming Tablets in Diabetic Retinopathy

Mengmeng Yang[1,*], Hualin Liu[1,*], Jiewen Zhou[2,*], Kewei Wang[1], Yujing Sun[1], Na Ning[3], Qiuling Huang[3], Jiajia Hu[3,4], Jidong Liu[1,5–7], Fei Yan[1,5–7], Xinguo Hou[1,5–7], Li Chen[1,5–7], Lingshu Wang[1,5–7], Fuqiang Liu[1,5–7]

[1]Department of Endocrinology, Qilu Hospital of Shandong University, Jinan, Shandong, 250000, People's Republic of China; [2]The First Affiliated Hospital, Guangzhou University of Chinese Medicine, Guangzhou, Guangdong, 510000, People's Republic of China; [3]Guangzhou Baiyunshan Zhongyi Pharmaceutical Co., Ltd, Guangzhou, Guangdong, 510000, People's Republic of China; [4]Wenzhou Medical University, Wenzhou, Zhejiang, 325000, People's Republic of China; [5]Institute of Endocrine and Metabolic Diseases of Shandong University, Jinan, Shandong, 250000, People's Republic of China; [6]Key Laboratory of Endocrine and Metabolic Diseases, Shandong Province Medicine & Health, Jinan, Shandong, 250000, People's Republic of China; [7]Jinan Clinical Research Center for Endocrine and Metabolic Disease, Jinan, Shandong, 250000, People's Republic of China

*These authors contributed equally to this work

Correspondence: Fuqiang Liu; Lingshu Wang, Department of Endocrinology, Qilu Hospital of Shandong University, Jinan, Shandong, 250000, People's Republic of China, Email liufuqiang@sdu.edu.cn; wanglingshu@qiluhospital.com

Background: Zhangyanming Tablets (ZYMT) is a proprietary Chinese medicine containing a variety of traditional Chinese medicines, which can be used to treat a wide range of eye diseases, but its exact effect on diabetic retinopathy (DR) and the specific mechanism are still unclear. This study aims to investigate the ameliorative effects and specific mechanisms of ZYMT on DR.

Methods: Key regulatory genes and potential therapeutic targets of ZYMT for DR were evaluated using network pharmacological analysis. Diabetic db/db mice were given low-dose ZYMT (330 mg/kg) and high-dose ZYMT (660 mg/kg), and relevant metabolic indices were tested. Histochemical staining and optical coherence tomography angiography (OCTA) were used to evaluate the histopathological structure of mice retina, RT-qPCR, TUNEL staining and immunofluorescence staining were used to evaluate the anti-apoptosis and anti-angiogenesis effect of ZYMT on DR.

Results: The results of network topology analysis showed that the top 10 Traditional Chinese Medicine (TCM) ingredients of ZYMT were quercetin, luteolin, kaempferol, wogonin, naringenin, β-sitosterol, baicalein, isorhamnetin, acacetin, and stigmasterol. ZYMT treats DR through key nodes such as AKT1, TNF, MAPK8, RELA, VEGFA, HIF1A, IL6, CASP3, BCL2, STAT3, and ICAM1. ZYMT has a direct effect on DR rather than secondary improvement of metabolic indices. Tissue staining demonstrated that ZYMT improved retinal vascular morphology and delayed retinal thinning in db/db mice. The OCTA imaging also showed that ZYMT increased blood flow density in db/db mice. TUNEL staining and RT-qPCR results showed that ZYMT could reduce the apoptosis of retinal cells in db/db mice, and RT-qPCR and immunofluorescence staining showed that ZYMT could inhibit retinal neovascularization.

Conclusion: This study found the potential target of ZYMT to ameliorate DR through network pharmacological analysis, and verified that ZYMT can improve DR by exerting anti-apoptosis and anti-neovascularization.

Keywords: diabetic retinopathy, zhangyanming tablets, network pharmacological analysis, apoptosis, neovascularization

Introduction

Diabetes mellitus (DM) is a group of chronic metabolic diseases characterized by hyperglycemia, the number of patients with DM continues to increase at an alarming rate, and it is estimated that the global incidence will reach 5.4% by 2025.[1] Prolonged hyperglycemia can lead to microvascular complications, resulting in diabetic nephropathy, diabetic retinopathy

Received: 9 September 2024
Accepted: 14 April 2025
Published: 28 April 2025

© 2025 Yang et al. This work is published and licensed by Dove Medical Press Limited. The full terms of this license are available at https://www.dovepress.com/terms.php and incorporate the Creative Commons Attribution – Non Commercial (unported, v4.0) License (http://creativecommons.org/licenses/by-nc/4.0/). By accessing the work you hereby accept the Terms. Non-commercial uses of the work are permitted without any further permission from Dove Medical Press Limited, provided the work is properly attributed. For permission for commercial use of this work, please see paragraphs 4.2 and 5 of our Terms (https://www.dovepress.com/terms.php).

(DR), and diabetic peripheral neuropathy. DR is the leading cause of new cases of blindness in adults aged 20–74 years.[2] The global prevalence of DR was 103 million in 2020 and is projected to rise to approximately 130 million in 2030 and 161 million in 2045.[3] DR not only severely impairs the quality of life and survival of patients but also imposes a serious economic burden on society. Therefore, identifying effective treatments for DR is imperative.

DR can be categorized into non-proliferative diabetic retinopathy (NPDR) and proliferative diabetic retinopathy (PDR).[4] NPDR is the early stage of DR, characterized by microaneurysms, small hemorrhagic dots, hard exudates, and soft exudates, and treatments include pharmacologic intervention and laser therapy. PDR is a more severe stage of DR characterized by neovascularization, vitreous hemorrhages, fibroproliferative membranes, and tractional retinal detachment, which may require surgical treatment.[5] Retinal laser photocoagulation and surgery are both invasive treatments, total retinal laser photocoagulation is associated with changes in visual field narrowing and requires more than 2 surgeries to maintain good retinal condition, and vitrectomy is only indicated for advanced diabetic lesions and is not advantageous in treating early-stage lesions.[6] Therefore, the therapeutic goal is to control DR in the non-proliferative stage and hope to achieve a satisfactory outcome with pharmacologic intervention.

In recent years, the discovery of DR therapeutic drugs with good efficacy and low toxicity and side effects from Traditional Chinese Medicine (TCM) resources has become a research hot spot. Numerous studies have shown that TCM and their extracts have remarkable effects on multiple pathogenic mechanisms of DR and application value in preventing or delaying DR.[7] Zhangyanming Tablets (ZYMT) is a proprietary Chinese medicine that can be used to treat cataracts and has been widely used in clinical practice for over 40 years. ZYMT contains 22 Chinese medicinal herbs, including Rhizoma Acori Tatarinowii, Semen Cassiae, Herba Cistanches, Radix Puerariae Lobatae, Semen Celosiae, and Radix Codonopsis, etc.[8] ZYMT can be used to treat the symptoms of dryness and astringency caused by insufficiency of the liver and kidney, monocularity, lumbar and knee soreness, diplopia, mild vision loss, and early and middle age cataract. A recent study found that ZYMT had a protective effect in a mouse model of retinitis pigmentosa,[8] demonstrating that ZYMT can also improve other ocular diseases.

Accumulating studies have shown that multiple pathological mechanisms are jointly involved in the pathogenesis of DR, including oxidative stress, abnormalities in polyol metabolic pathways, aberrant aggregation of late-stage glycosylation end-products, impairment of proteinase C signaling pathways, and inflammatory responses.[9] Among these, aldose reductase, the main enzyme in the polyol pathway, catalyzes the conversion of glucose to sorbitol, leading to a significant buildup of reactive oxygen species (ROS) in different tissues.[1,10] The role of chronic low-grade inflammatory response and oxidative stress in the pathogenesis of DR has received significant research attention. Inflammatory response triggers functional impairment of Müller cells, which in turn leads to reduced glutamate recycling by Müller cells, further triggering retinal ganglion cell dysfunction and apoptosis.[11] Inhibition of inflammatory signaling pathways attenuates the inflammatory response of retinal endothelial cells and reduces disruption of the blood-retinal barrier. The retina is one of the highest oxygen-consuming tissues in the body and is therefore more susceptible to attack by ROS. Excessive production of ROS leads to elevated retinal oxidative stress and mitochondrial dysfunction, which in turn causes a series of retinal tissue cellular function impairments such as retinal capillary cell apoptosis.[9] Studies have reported that various components in ZYMT, such as puerarin and astragalus, have anti-inflammatory and anti-oxidative stress effects,[12,13] which suggests that ZYMT may play a potential therapeutic role in DR.

The present study sought to elucidate the effect and underlying mechanism of ZYMT in DR mice. The network pharmacological method was used to construct the "ZYMT- components-targets-DR" network to predict and analyze the intrinsic mechanism by which ZYMT treats DR, which was validated in vivo using diabetic db/db mice. This study explores the potential of ZYMT to improve DR and provides a safe, convenient, and effective alternative strategy for the clinical treatment of DR.

Methods

The Method of Fingerprint Analysis of ZYMT

Chromatographical analysis was conducted on Waters e2695 hPLC platform (integrating degasser unit, auto sampler unit, column thermostat), equipped with Diode Array Detector (DAD), following previous research.[8] Methanol (HPLC grade) was purchased from Sigma-Aldrich (USA). Purified water was produced using Milli-Q system (Millipore, USA).

Puerarin (200912), cynaroside (202111), echinacoside (200502), verbascoside (201713) and linarin (200606) were purchased from National Institute for Food and Drug Control. 3'-Methoxypuerarin (CHB180325), 3'-hydroxypuerarin (CHB170224) and puerarin apioside (CHB180620) were obtained from Chroma-Biotechnology Co., Ltd (Chengdu, China). Puerarin 6'-O-xyloside (B20447) was obtained from Yuanye Bio-Technology Co., Ltd (Shanghai, China).

Four batches of ZYMT were used in this study, namely, (C02001, C04002, Z04003, Y04004). Specimens of ZYMT were deposited in Department of Endocrinology, Qilu Hospital of Shandong University.

ZYMT (2.0 g) was powdered, weighed, and then extracted under ultrasound (300 W, 40 kHz) with 75% methanol (20 mL). Solvent was collected after filtration. Samples (10 μm) were subjected to separation using Hypersil ODS2 column (250 mm × 4.6 mm, 5 μm, Elite Analytical Instruments, China). Mobile phase consists of water (A) and methanol (B). Gradient elution was set as followed, 0−12 min, 5% B; 12−25 min, 5–20% B; 25−50 min, 20–27% B; 50 −57 min, 27–32% B; 57−75 min, 32–33% B; 75−80 min, 33–42% B; 80−85 min, 42−45% B; 85−100 min, 45% B; 100−105 min, 45–60% B; 105−110 min, 60–80% B; 110−120 min, 80–90% B. The flow rate was kept at 1 mL/min. The column temperature was held constant at 35°C. DAD parameters were as followed, 0~16 min, 280 nm; 16~46 min, 254 nm; 46~75 min, 220 nm; 75~120 min, 254 nm.

Collection of Active Ingredients and Target Prediction of ZYMT

The Traditional Chinese Medicine Systems Pharmacology Database and Analysis Platform (TCMSP) database was searched for Rhizoma Acori Tatarinowii, Herba Cistanches, Semen Celosiae, Fructus Viticis, Semen Plantaginis, Fructus Corni, Semen Cuscutae, Nux Prinsepiae, Flos Buddlejae, Rhizoma Polygonati, Cortex Phellodendri Amurensis, Semen Cassiae, Radix Puerariae Lobatae, Radix Codonopsis, Fructus Lycii, Radix Paeoniae Alba, Radix et Rhizoma Glycyrrhizae, Rhizoma Cimicifugae, Flos Chrysanthemi, Rhizoma Chuanxiong, Radix Rehmanniae Praeparata and Radix Astragali (detailed formula of ZYMT, see Table 1). Active compounds were screened based on oral bioavailability (OB) ≥ 30% and drug-likeness (DL) ≥ 0.18. The target gene information of the drugs was obtained from the TCMSP and UniProt databases.

Acquisition of Potential Targets for DR

The GeneCards, DisGeNET, and Online Mendelian Inheritance in Man (OMIM) databases were searched using the keyword "diabetic retinopathy" to identify potential targets of the disease. Targets with a Relevance score ≥ median was screened in the GeneCards database to obtain potential targets for DR.

Construction of the "ZYMT-Active Ingredient-Disease-Drug Intersection Target" Network

After drawing the Venn diagram using the jvenn tool, the intersection targets of the drugs were obtained and the "Traditional Chinese Medicine-Component-Target Map" was constructed using Cytoscape 3.8.2. Targets with Betweenness Centrality, Closeness Centrality, and Degree greater than their median were selected as the core nodes of the network.

Construction of Protein Interaction Network Maps

The Search Tool for Retrieval of Interacting Genes/Proteins (STRING) platform was applied to construct the protein-protein interaction network (PPI) of disease-drug intersection targets, with the lowest interaction threshold set to 0.4, isolated nodes hidden, and the rest as default values. The data results were imported into Cytoscape 3.8.2 for network analysis. Nodes indicate different targets, and edges indicate the relationship between different targets.

Gene Ontology (GO) and Kyoto Encyclopedia of Genes and Genomes (KEGG) Pathway Enrichment Analyses

The disease-drug intersection targets were imported into the Database for Annotation, Visualization, and Integrated Discovery (DAVID) database, "select identifier" was set as the "official gene symbol", "list type" as "genelist", and species as "homo sapiens", and then perform GO pathway enrichment analysis and KEGG pathway enrichment analysis respectively.

Table 1 Natural Medicines in the Formula of Zhangyanming Tablets and Their Origins

Natural Medicine	Origin of Natural Medicine
Rhizoma Acori Tatarinowii	*Acorus tatarinowii* Schott
Herba Cistanches	*Cistanche deserticola* Y. C. Ma
Semen Celosiae	*Celosia argentea* L.
Fructus Viticis	*Vitex trifolia* L.
Semen Plantaginis	*Plantago asiatica* L.
Fructus Corni	*Cornus officinalis* Sieb. et Zucc.
Semen Cuscutae	*Cuscuta Chinensis* Lam.
Nux Prinsepiae	*Prinsepia uniflora* Batal.
Flos Buddlejae	*Buddleja officinalis* Maxim.
Rhizoma Polygonati	*Polygonatum sibiricum* Red.
Cortex Phellodendri Amurensis	*Phellodendron amurense* Rupr.
Semen Cassiae	*Cassia obtusifolia* L.
Radix Puerariae Lobatae	*Pueraria lobata* (Willd.) Ohwi
Radix Codonopsis	*Codonopsis pilosula* (Franch.) Nannf.
Fructus Lycii	*Lycium barbarum* L.
Radix Paeoniae Alba	*Paeonia lactiflora* Pall.
Radix et Rhizoma Glycyrrhizae	*Glycyrrhiza uralensis* Fisch.
Rhizoma Cimicifugae	*Cimicifuga foetida* L.
Flos Chrysanthemi	*Chrysanthemum morifolium* Ramat.
Rhizoma Chuanxiong	*Ligusticum chuanxiong* Hort.
Radix Rehmanniae Praeparata	*Rehmannia glutinosa* (Gaertn.) DC.
Radix Astragali	*Astragalus membranaceus* (Fisch.) Ege.

Abbreviations: ZYMT, Zhangyanming tablets; DR, diabetic retinopathy; IPGTT, intraperitoneal glucose tolerance test; ELISA, enzyme-linked immunosorbent assay; OCTA, optical coherence tomography angiography; RT-qPCR, real-time quantitative PCR; TCM, Traditional Chinese Medicine; DM, diabetes mellitus; NPDR, non-proliferative diabetic retinopathy; PDR, proliferative diabetic retinopathy; ROS, reactive oxygen species; TCMSP, Traditional Chinese Medicine Systems Pharmacology Database and Analysis Platform; OB, bioavailability; DL, drug-likeness; OMIM, Online Mendelian Inheritance in Man; STRING, Search Tool for Retrieval of Interacting Genes/Proteins; PPI, protein-protein interaction network; GO, Gene Ontology; KEGG, Kyoto Encyclopedia of Genes and Genomes; TG, triglyceride; LDL, low-density lipoprotein; HDL, high-density lipoprotein; CHO, cholesterol; HE, hematoxylin and eosin; PAS, periodic acid-Schiff; CD31, cluster of differentiation 31; HIF-1α, hypoxia-inducible factor 1-alpha; VEGF, vascular endothelial growth factor; BPs, biological processes; FDR, false discovery rate; AKT1, serine/threonine kinase 1; MAPK8, mitogen-activated protein kinase 8; AGE, advanced glycation end product; NF-κB, nuclear factor-kappa B; TNF-α, tumor necrosis factor-alpha; IL-1β, interleukin-1 beta; BCL-2, B-cell lymphoma-2; BAX, BCL2 associated X; Dll4, delta-like ligand 4.

Molecular Docking Validation of Active Ingredient and Key Targets

To further validate the affinity of the active ingredients with the targets of disease-drug intersection, the active ingredient screened from the network diagram of Traditional Chinese Medicine-Component-Target Map were selected, and their sdf structural formulae were downloaded from the pubchem database as the drug small molecules, and the 3D structural formulae of disease-drug intersection targets were obtained by searching the Protein Structure Data Bank (PDB) as the protein macromolecules. PyMOL software was used to complete the processing of protein receptor structure to remove water molecules and invalid small molecule ligands. The target proteins and drug active ingredients were imported into AutoDock Tools 1.5.7, and the semi-flexible docking of molecules was performed using AutoDock Vina to obtain the binding energy and binding position of the active molecule with the receptor protein.[14]

Animals

Four-week-old male db/db mice were purchased from Jiangsu Jicui Biotechnology Co., Ltd. (Jiangsu, China). Mice were raised in the Animal Center of Qilu Hospital of Shandong University. Mice were maintained at a temperature of 25 ± 5°C and humidity of 60 ± 5%, with *ad libitum* access to water and feed. This study has been approved by the Experimental Animal Ethics Committee of Qilu Hospital of Shandong University (ethics approval number: DWLL-2022-071), complying with the Regulations on the Administration of Experimental Animals of Shandong Province (dated

January 24, 2018). The diabetic mouse model was established after two consecutive measurements of tail-tip blood glucose values ≥16.7 mmol/L. Due to the short study duration, only early-stage DR mice were analyzed. Db/db mice were divided into three groups: the db/db + vehicle group, the db/db + low-dose ZYMT group (330 mg/kg), the db/db + high-dose ZYMT group (660 mg/kg). ZYMT was prepared in a vehicle (corn oil) and administered by tube feeding once daily for 7 weeks. The proportion of ZYMT and corn oil was adjusted according to the dosage group: 33 mg/mL for the low dose group (330 mg/kg) and 66 mg/mL for the high dose group (660 mg/kg). The daily gastric perfusion volume is determined according to the weight of mice, for example, the weight of mice is X g and the gastric perfusion volume is 0.01X mL. The gastric perfusion volume conforms to the animal ethics (less than 10 mL/kg). The solubility stability of ZYMT in corn oil was verified by pre-experiments, and no precipitation or stratification was observed. The nondiabetic control group (db/m mice) and the db/db + vehicle group were given an equal volume of the vehicle without ZYMT. Mice were tested weekly for fasting blood glucose and body weight, and intraperitoneal glucose tolerance test (IPGTT) experiments were performed a week after the end of the intervention. Mice were anesthetized and then executed. Subsequently, serum was collected, the left eye tissue was fixed with paraformaldehyde, and the retina was stripped from the right eye tissue and frozen in a −80°C refrigerator until use.

Intraperitoneal Glucose Tolerance Test (IPGTT)

All mice were fasted overnight and injected intraperitoneally with glucose solution. The tail-tip blood was collected at 0, 30, 60, 90, 120, and 150 minutes after injection to measure blood glucose values.

Serum Index Detection

Serum insulin level, triglyceride (TG), low-density lipoprotein (LDL), high-density lipoprotein (HDL) and cholesterol (CHO) were measured using the Enzyme-linked immunosorbent assay (ELISA) kits according to the manufacturer's instructions.

Hematoxylin and Eosin (HE) Staining

Paraformaldehyde pre-fixed retinal tissues were paraffin-embedded and sliced into 3-μm-thick sections. After a rigorous dewaxing, standard HE staining was performed, followed by observation under a light microscope.

Periodic Acid-Schiff (PAS) Staining

Retinal vascular lesions were visualized using PAS staining as previously described.[15]

Optical Coherence Tomography Angiography (OCTA)

After the intervention of ZYMT, all mice were examined by OCTA. At first, the pupil of mice was dilated with tropicamide solution, and the mice were anesthetized by intraperitoneal injection of tribromoethanol solution. After that, the mice were placed on UWF SS-OCTA equipment for binocular detection (Towerpi Medical Technology Co., Ltd., Beijing, China, Machine Model: BM400K BMizar). After the examination, the blood flow density and retinal thickness were analyzed by OCTFunduslmage3 software.

Real-Time Quantitative PCR (RT-qPCR)

Right retinal tissue RNA was extracted using Trizol reagent, and the concentration and purity of RNA were determined using an ultraviolet spectrophotometer. RNA was transcribed into complementary DNA using the Prime Script RT Reagent Kit according to the manufacturer's instructions, and RT-qPCR reactions were performed using the SYBR Green PCR Kit. Gene expression was calculated using the $2^{-\Delta\Delta Ct}$ method and quantified using *β-actin* as a reference. Nucleotides were supplied by Shanghai Jimma, and primer sequences were as follows: *Bcl-2*, sense 5'-TTCAGGGATGGGGTGAACTG-3' and antisense 5'-CACAGGGCGATGTTGT-3'; *Bax*, sense 5'-CCCGAGAGGTCTTCTTCC-3' and antisense 5'-GCCTTGAGCACCAGTTTG-3'; *Vegf*, sense 5'-GCTACTGCCGTCCGATTGA-3' and antisense 5'-ATGGTGATGTTGCTCTCTGA-3'; *Hif-1α*, sense 5'-ACCTTCATCGGAAACTCCAAAG-3' and antisense 5'- CTGTTAGGCTGGGAAAAGTTAGG-3'; *Cd31*, sense 5'-

ACGCTGGTGCTCTATGCAAG-3' and antisense 5'- TCAGTTGCTGCCCATTCATCA-3'; *Notch-1*, sense 5'-CACACCCCTCATGATTGCCT-3' and antisense5'-GTCCAGCAACACTTTGGCAG-3'; *Dll-4*, sense 5'-AGCTGGGTGTCTGAGTAGGC −3' and antisense 5'-AGAAGGTGCCACTTCGGTTA-3'; *β-actin*, sense 5'-GTGACGTTGACATCCGTAAAGA-3' and antisense 5'-GCCGGACTCATCGTACTCC-3'.

Immunofluorescence Staining

Retinal paraffin sections were first deparaffinized according to standard procedures, then antigenically repaired using citrate buffer, immediately followed by sealing with goat serum for 30 min. Sections were co-incubated at 4°C overnight with primary antibodies against cluster of differentiation 31 (CD31, 1:100, Abcam, USA, ab222783), hypoxia-inducible factor 1-alpha (HIF-1α, 1:100, Abcam, USA, ab179483), and vascular endothelial growth factor (VEGF, 1:50, ABclonal, China, A5708). On the next day, sections were co-incubated with a fluorescent secondary antibody at room temperature for 1 h. Finally, fluorescent signals were observed under a fluorescence microscope.

TUNEL Staining

Retinal cell apoptosis was detected using the In Situ Cell Death Detection Kit (Roche, USA) according to the manufacturer's instructions.

Statistical Analysis

All experiments were performed in triplicate. Data were presented as mean ± SD and analyzed using GraphPad 8.0 software. The *t*-test was applied to compare statistical differences between two groups, whereas one-way ANOVA was used for comparing multiple groups. $P < 0.05$ was considered statistically significant.

Results

The Quality Control of ZYMT

The voucher specimens of Zhangyanming Tablets (C02001, C04002, Z04003, Y04004) in this study were kept in Department of Endocrinology, Qilu Hospital of Shandong University (Guangzhou Baiyunshan Zhongyi Pharmaceutical Co., Ltd). Representative fingerprint chromatography profiles were shown in Figure 1. And Peak 1, 2, 3, 4, 5, 6, 7, 8 and

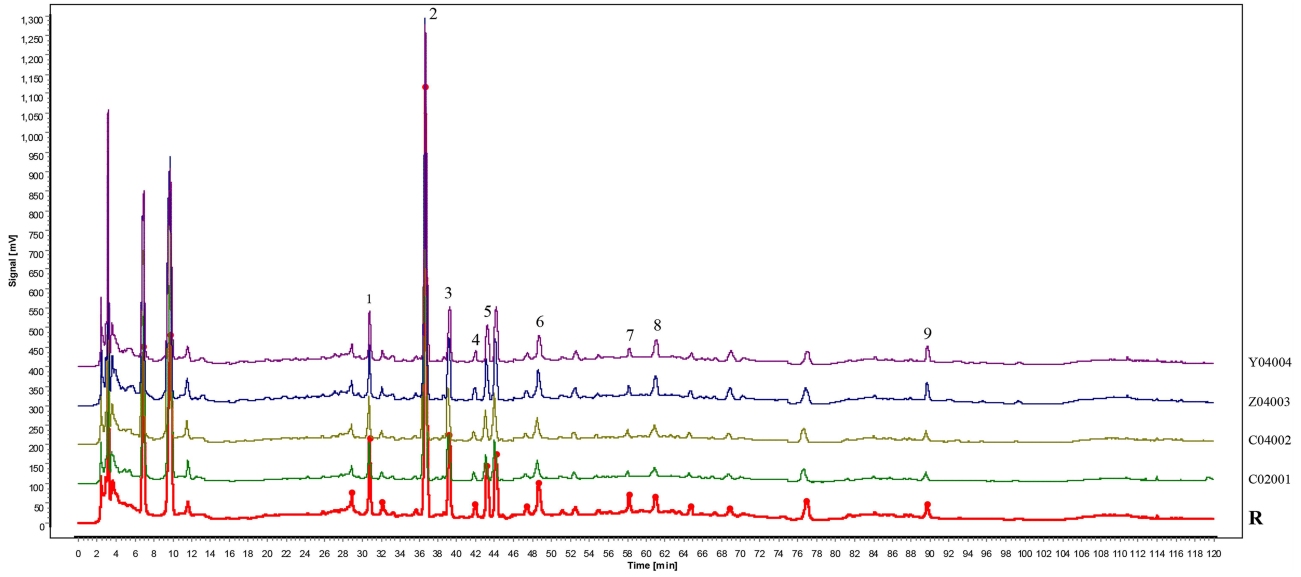

Figure 1 Four batches of fingerprint analysis of ZYMT. Compounds were identified using standard reference, (1)-3'-hydroxypuerarin, (2)-puerarin, (3)-3'-methoxypuerarin, (4)-puerarin 6"-O-xyloside, (5)-puerarin apioside, (6)-echinacoside, (7)-verbascoside, (8)-cynaroside, (9)-linarin. (R) reference fingerprint chromatogram.

9 were identified as 3'-hydroxypuerarin, puerarin, 3'-methoxypuerarin, puerarin 6"-O-xyloside, puerarin apioside, echinacoside, verbascoside, cynaroside and linarin, respectively.

Network Pharmacological Results

Acquisition of Potential Targets of TCMs

After OB and DL screening, the following active ingredients were obtained from the TCMSP database: Rhizoma Acori Tatarinowii (4), Semen Cassiae (14), Herba Cistanches (6), Radix Puerariae Lobatae (4), Semen Celosiae (2), Radix Codonopsis (21), Fructus Viticis (27), Fructus Lycii (45), Semen Plantaginis (9), Radix Paeoniae Alba (13), Fructus Corni (20), Radix et Rhizoma Glycyrrhizae (92), Semen Cuscutae (11), Rhizoma Cimicifugae (17), Nux Prinsepiae (7), Flos Chrysanthemi (20), Flos Buddlejae (4), Rhizoma Chuanxiong (7), Rhizoma Polygonati (12), Radix Rehmanniae Praeparata (2), Cortex Phellodendri Amurensis (30), and Radix Astragali (20). A total of 256 potential TCM targets were obtained after merging and de-emphasizing.

Acquisition of Potential Disease Targets

Overall, 3431 DR-related targets were obtained from various databases, including 2598 from the GeneCards database, 645 from the DisGeNET database, and 188 from the OMIM database, of which 2926 were retained after merging and de-emphasizing.

Construction of the "Traditional Chinese Medicine-Component-Disease-Drug Intersection Targets" Network

A Venn diagram of potential drug targets and disease targets was drawn, and an intersection of ZYMT and DR was obtained (Figure 2A). The "traditional Chinese medicine-component-target network graph" was constructed (Figure 2B), in which there were 22 drug nodes, 202 ingredient nodes, and 141 disease-drug intersection targets. According to the results of the network topology analysis, the top 10 TCM active ingredients in the core nodes of this network were quercetin, luteolin, kaempferol, wogonin, naringenin, β-sitosterol, baicalein, isorhamnetin, acacetin, and stigmasterol.

PPI Network Construction

The STRING platform was utilized to construct a PPI network of disease-drug intersection targets (Figure 3A). In the PPI network graph, there are 140 nodes and 3066 edges. After filtering according to the network topology attribute values, the top 10 targets of this network with degree values were sequentially AKT1, TNF, IL6, TP53, IL1B, EGFR, CASP3, MMP9, BCL2, and HIF1A.

GO and KEGG Pathway Enrichment Analyses

The results of GO enrichment analysis of 141 disease-drug intersecting targets yielded 713 biological processes (BPs), and the top 20 BPs in descending order of false discovery rate (FDR) value are shown in Figure 3B. Meanwhile, 175 pathways were obtained from the KEGG pathway enrichment analysis, and the top 18 pathways with more lower FDR values are displayed in Figure 3C.

Molecular Docking Validation of Active Ingredients and Key Targets

Human protein molecules were searched in PDB, and the molecules with smaller "method:X-RAY" and "resolution" in structure were selected as the sources of BCL2 and HIF1A protein molecules with PDB IDs of " 2w3l" and "4h6j", respectively. 2w3l" and '4h6j' were selected as the sources of BCL2 and HIF1A, respectively. The protein molecules were deleted from ligands, dehydrogenated and hydrogenated using pymol software, and the drug molecules were searched in the pubchem database. The protein molecules and drug molecules were imported into AutoDockTools-1.5.7, the docking box was set, and the molecules were docked using AutoDock Vina. The docked molecules are shown as heatmaps in Figure 3D. Preservation of conformations of drug molecules with low binding energies, co-imported with protein molecules into pymol for "docking site mapping" (Figure S1A-D).

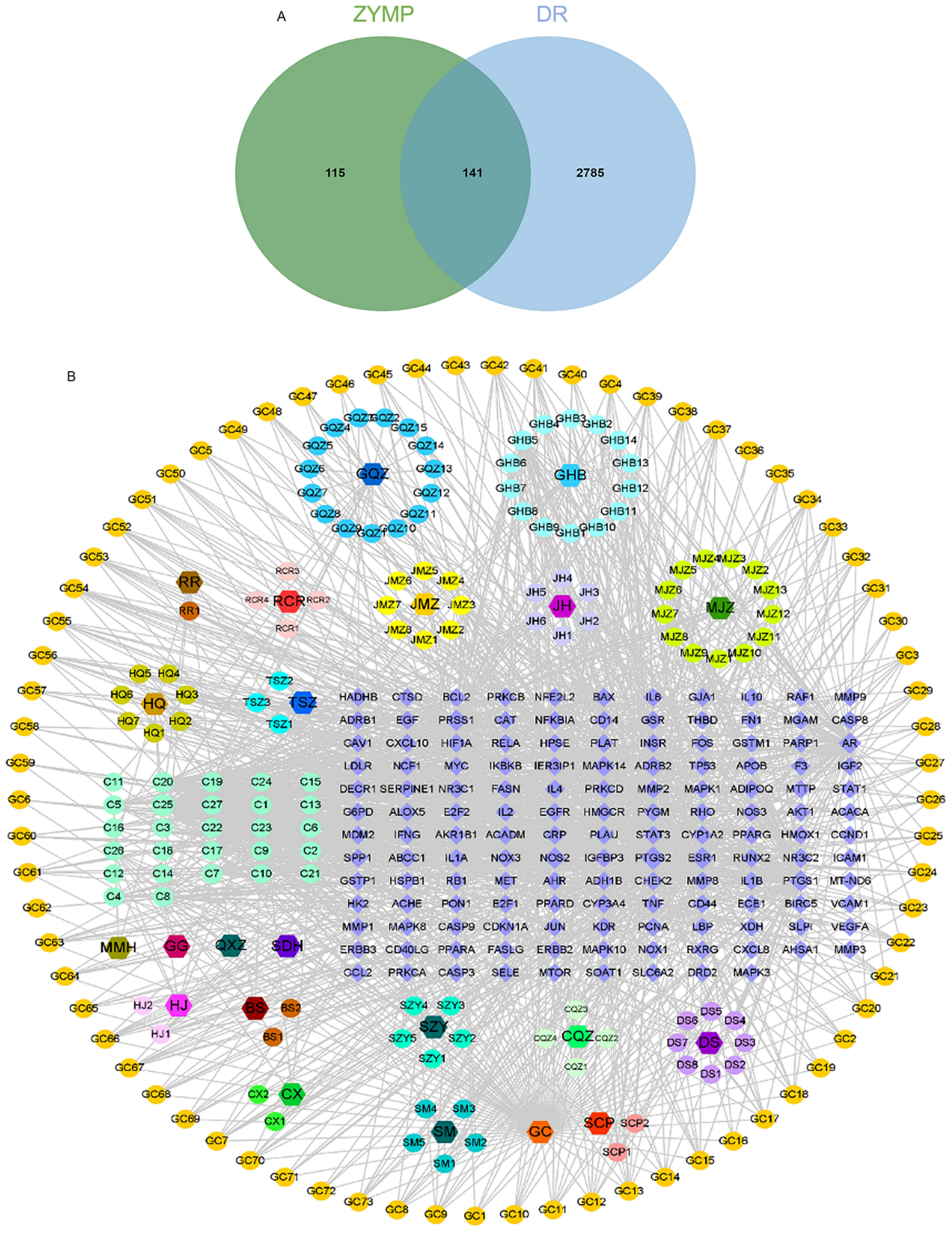

Figure 2 Construction of the "Traditional Chinese Medicine-component-disease-drug intersection targets" network. (**A**) Potential target points of ZYMT in treating DR, (**B**) Traditional Chinese Medicine-Component-Target" network diagram of ZYMT in treating DR.

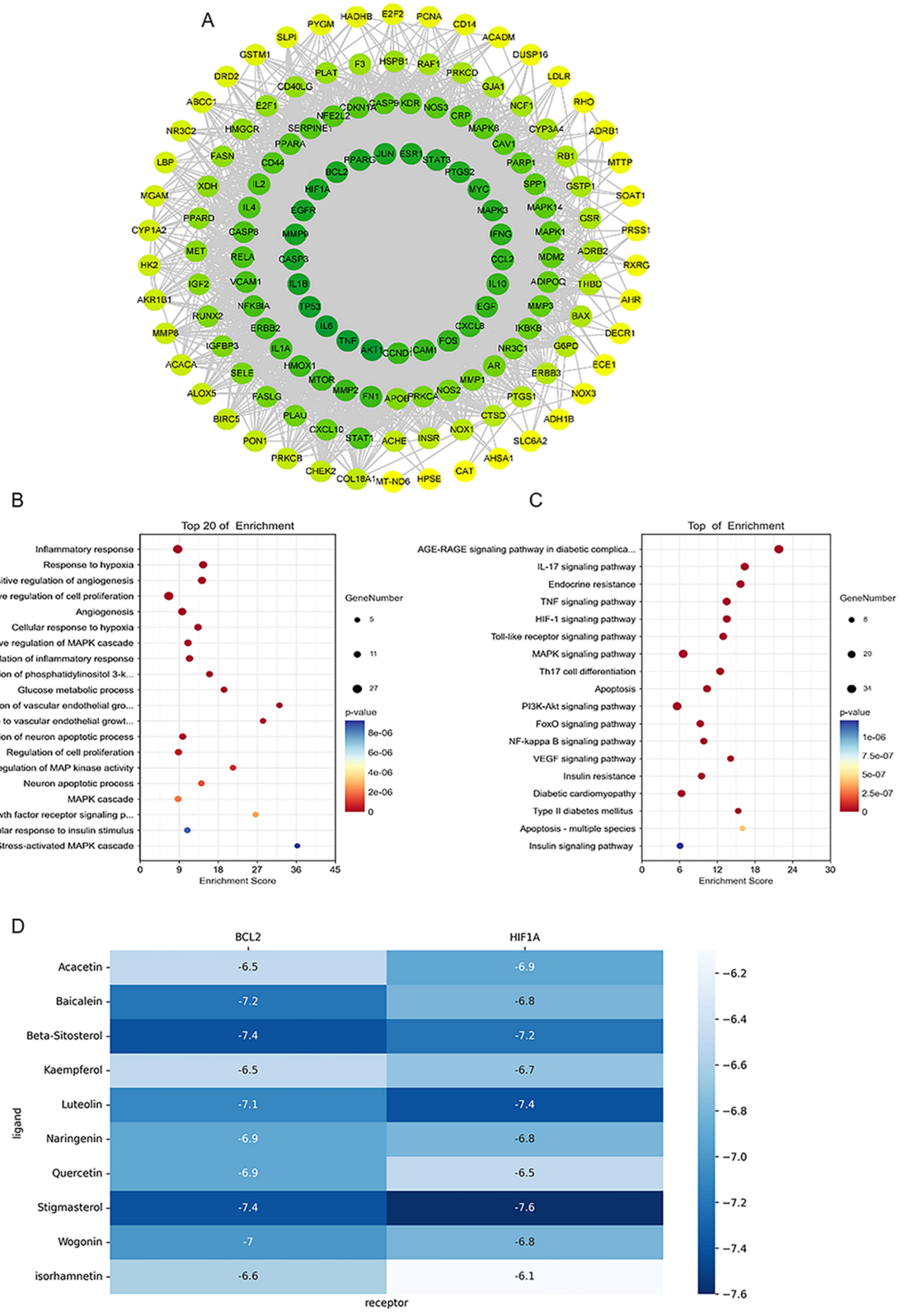

Figure 3 PPI network construction and GO and KEGG pathway enrichment analyses. (**A**) Protein-Protein Interaction (PPI) network diagram of disease-drug intersection target points in the treatment of DR with ZYMT. (**B**) Bubble Chart of GO Biological Process Enrichment Analysis. (**C**) Bubble Chart of KEGG Pathway Enrichment Analysis. (**D**) Binding energy of active components of ZYMT for molecular docking with BCL2 and HIF1A, respectively.

https://doi.org/10.2147/DMSO.S495286

Animal Results

Effect of ZYMT on Metabolic Indices in Db/Db Mice

Fasting blood glucose and body weight were significantly elevated in db/db mice compared with control mice. However. ZYMT treatment did not significantly affect the two indices (Figure 4A and B). In addition, the IPGTT assay showed that ZYMT did not improve glucose tolerance in db/db mice (Figure 4C). The serum insulin assay showed that ZYMT did not reduce elevated insulin levels in db/db mice (Figure 4D). Next, the effect of ZYMT on the lipid profile of db/db mice was examined and results showed that triglyceride (TG) and low-density lipoprotein (LDL) levels were significantly higher in db/db mice than in control mice, and the high-density lipoprotein (HDL) and cholesterol (CHO) levels of db/db mice were not significantly different from those of control mice. However, no significant change was detected in the lipid levels of db/db mice after ZYMT treatment (Figure S2A-D). Taken together, these findings suggested that the metabolic indexes of db/db mice were not significantly improved by ZYMT, and the improvement of DR by ZYMT was due to the direct effect on the retina.

ZYMT Improves Retinal Structure in Db/Db Mice

The effects of ZYMT on the retina of db/db mice were assessed by the optical coherence tomography angiography (OCTA) imaging system. ZYMT treatment increased the decreased blood flow density and delayed retinal thinning in the

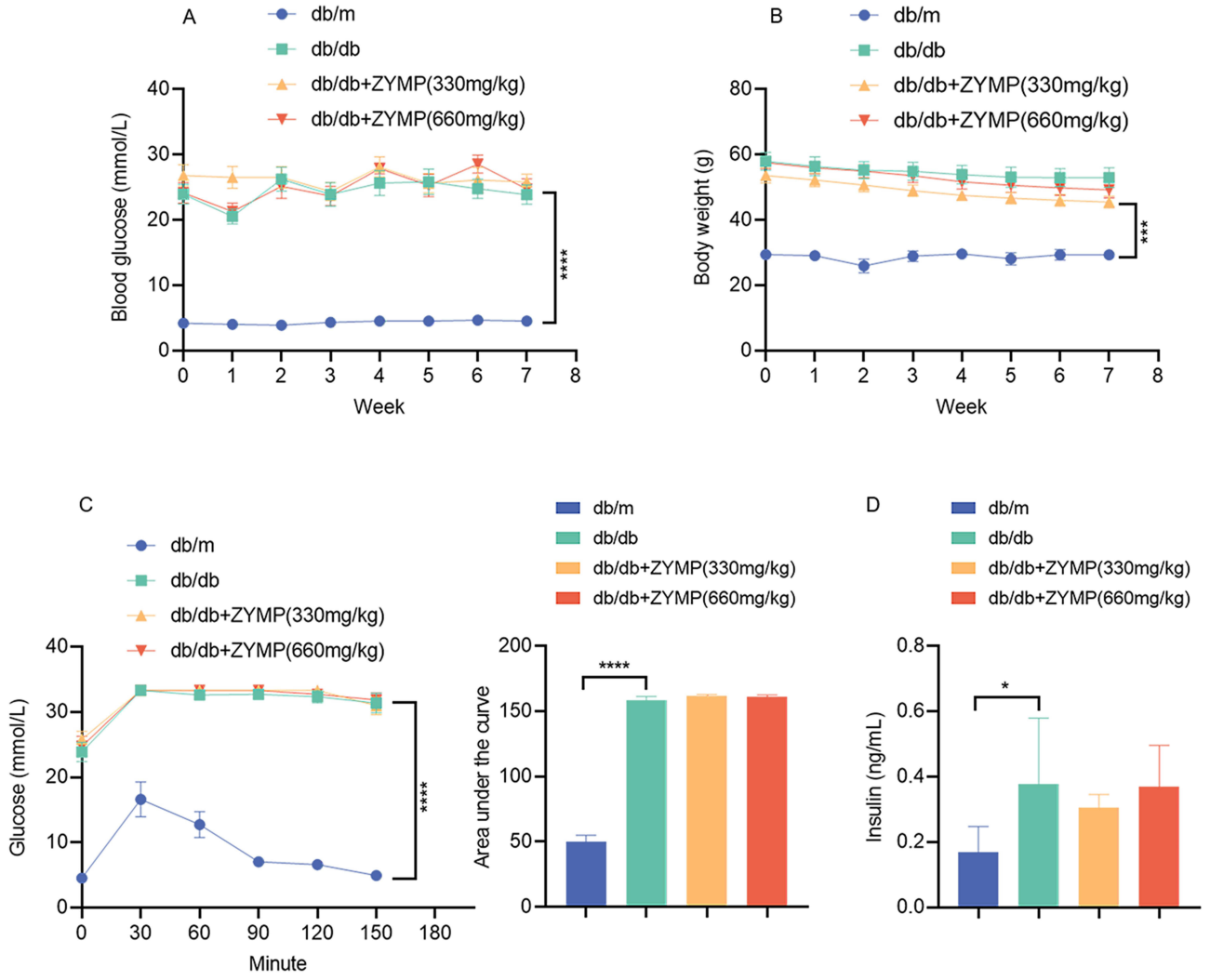

Figure 4 Effect of ZYMT on metabolic indices in db/db mice. (**A**) Glucose of mice in the db/m, db/db, db/db+ZYMT (330 mg/kg), and db/db+ZYMT (660 mg/kg) groups. (**B**) Body weights of mice. (**C**) Intraperitoneal glucose tolerance test (IPGTT) results and area under the curve. (**D**) Serum insulin levels in mice. Data are mean ± SD. *P<0.05, ***P<0.001, ****P<0.0001.

db/db mice (Figure 5A, Figure S2E and F). In addition, HE staining showed that the retinal thickness of db/db mice increased after ZYMT treatment, and the number of nuclei in INL and ONL increased significantly (Figure 5B). PAS staining revealed that db/db mice exhibited distorted and tangled retinal blood vessels, endothelial cell proliferation, pericyte reduction, and neovascularization, all of which were significantly inhibited by ZYMT (Figure 5C).

ZYMT Reduces Retinal Cell Apoptosis in Db/Db Mice

TUNEL staining showed that retinal apoptotic cells were significantly elevated in db/db mice, which were significantly reduced by ZYMT treatment (Figure 6A). Therefore, the effect of ZYMT on the expression of retinal apoptotic genes was examined. Results showed that the anti-apoptotic gene *Bcl-2* was significantly decreased and pro-apoptotic gene *Bax* was significantly upregulated in the retinas of db/db mice (Figure 6B and C). These effects were reversed by high-dose ZYMT treatment.

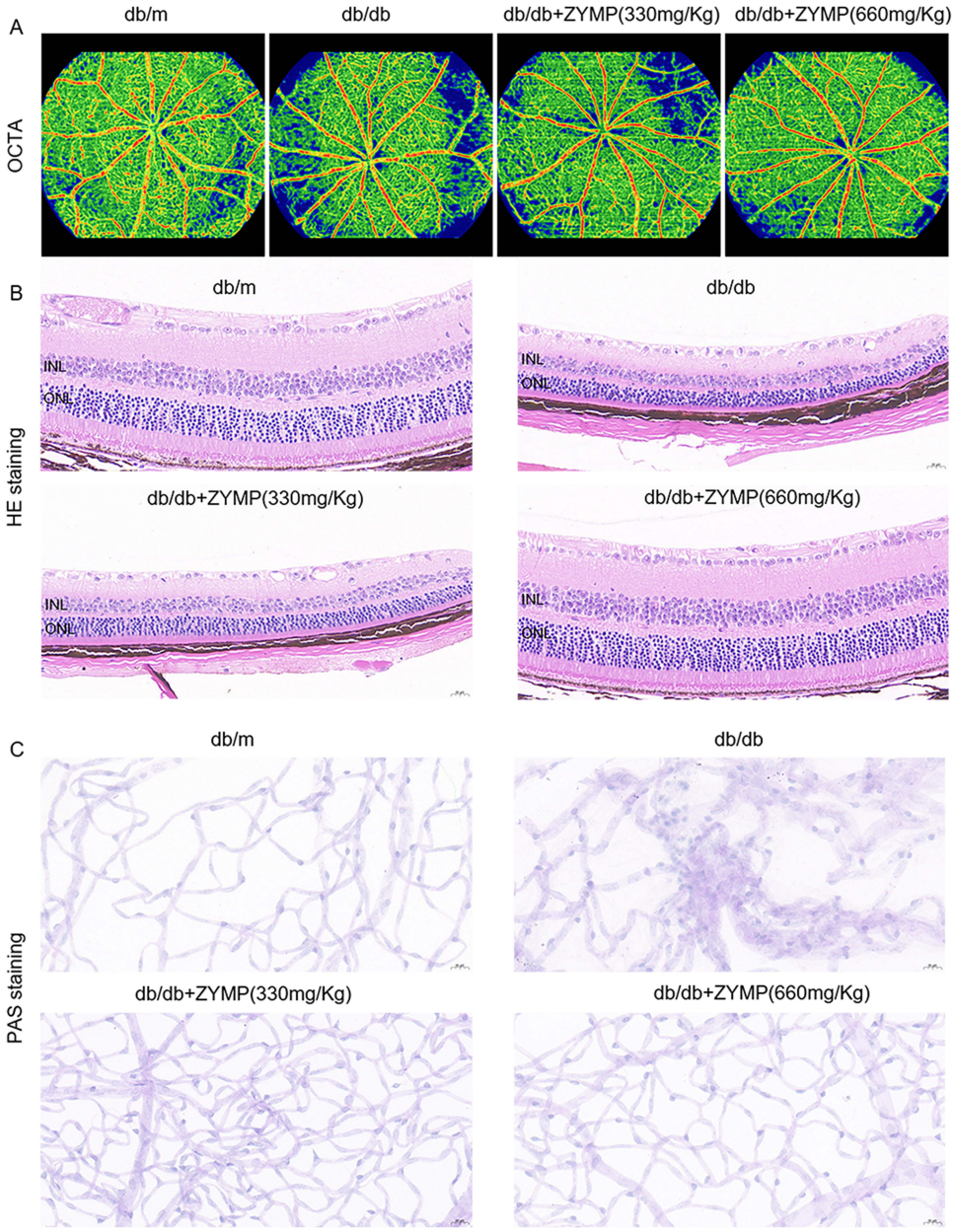

Figure 5 ZYMT improves retinal structure in db/db mice. (**A**) Representative image of retinal OCTA in control and db/db mice treated with vehicle or ZYMT. (**B**) HE staining. Scale Bar, 20 μm. (**C**) PAS staining. Scale Bar, 20 μm.

https://doi.org/10.2147/DMSO.S495286

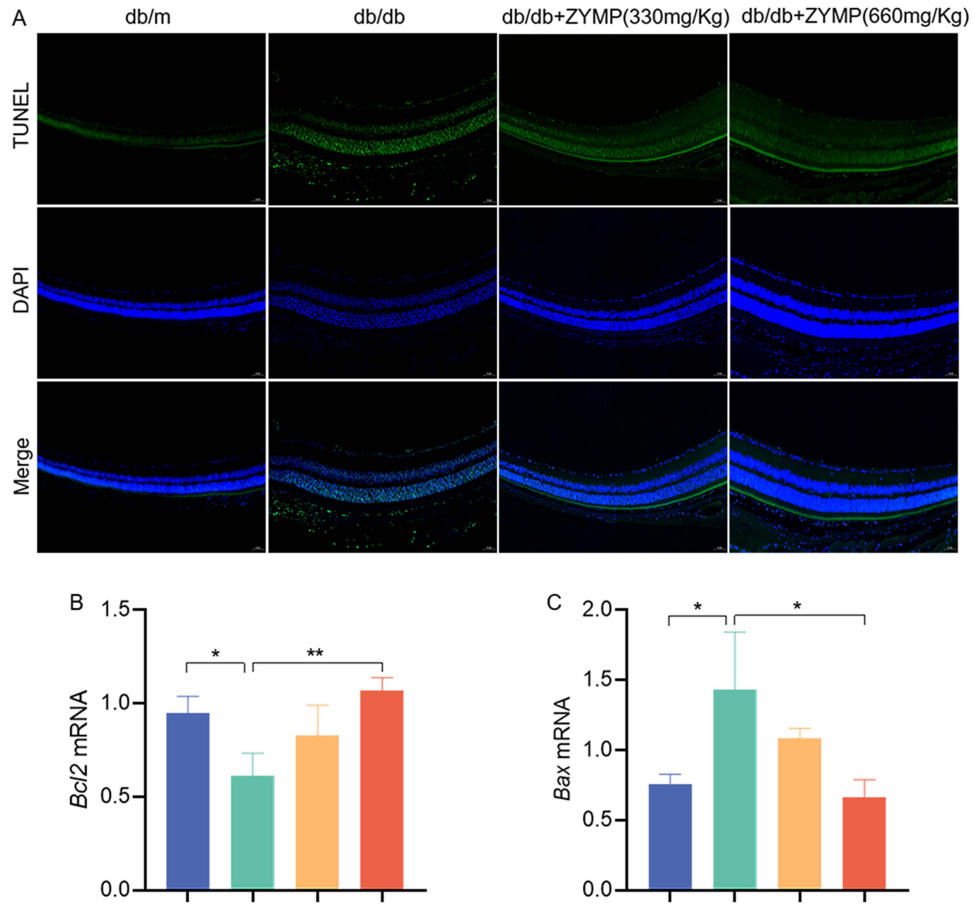

Figure 6 ZYMT reduces retinal cell apoptosis in db/db mice. (**A** and **B**). The mRNA levels of *Bcl-2* and *Bax* were determined by RT-qPCR. (**C**). TUNEL staining in control and db/db mice treated with vehicle or ZYMT. Data are mean ± SD. **P*<0.05, ***P*<0.01.

ZYMT Inhibits Neovascularization in Db/Db Mice

The effects of ZYMT on angiogenesis in db/db mice were also investigated. Messenger RNA (mRNA) levels of *Notch-1, Dll4, Cd31, Vegf*, and *Hif-1α* were determined, and all these vascular proliferation-related genes were significantly elevated in the db/db group and reduced after high-dose ZYMT treatment (Figure 7A-E). Immunofluorescence assays also demonstrated that ZYMT reduced the elevated expression of CD31, VEGF, and HIF-1α in the retinal tissues of db/db mice (Figure 8A-C).

Discussion

The present study analyzed 256 potential TCM targets, 2926 DR-related targets, and 141 common targets of ZYMT and DR using network pharmacological methods. The results of network topology analysis showed that the top 10 TCM ingredients were quercetin, luteolin, kaempferol, wogonin, naringenin, β-sitosterol, baicalein, isorhamnetin, acacetin, and stigmasterol. ZYMT treats DR through key nodes such as AKT1, TNF, MAPK8, RELA, VEGFA, HIF-1, IL6, CASP3, BCL2, STAT3, and ICAM1.

Serine/threonine kinase 1 (AKT1) is expressed in insulin-sensitive tissues and regulates glucose metabolism by inducing glucose transporter proteins to enhance glucose uptake.[16,17] The phosphoinositide 3-kinase (PI3K)-serine /threonine kinase (AKT) signaling pathway is activated in diabetes, and activated AKT causes vasodilatation, vascular remodeling, and neovascularization. Meanwhile, excessive angiogenesis leads to DR.[18] Mitogen-activated protein kinase 8 (MAPK8) gene belongs to the c-Jun N-terminal kinase (JNK)/MAPK pathway in the MAPK pathway, which is located in the advanced glycation end product (AGE)-receptor for AGE (RAGE) signaling pathway of diabetic complications and regulates cell growth, differentiation, apoptosis, etc.[19] The v-rel avian reticuloendotheliosis viral oncogene homolog

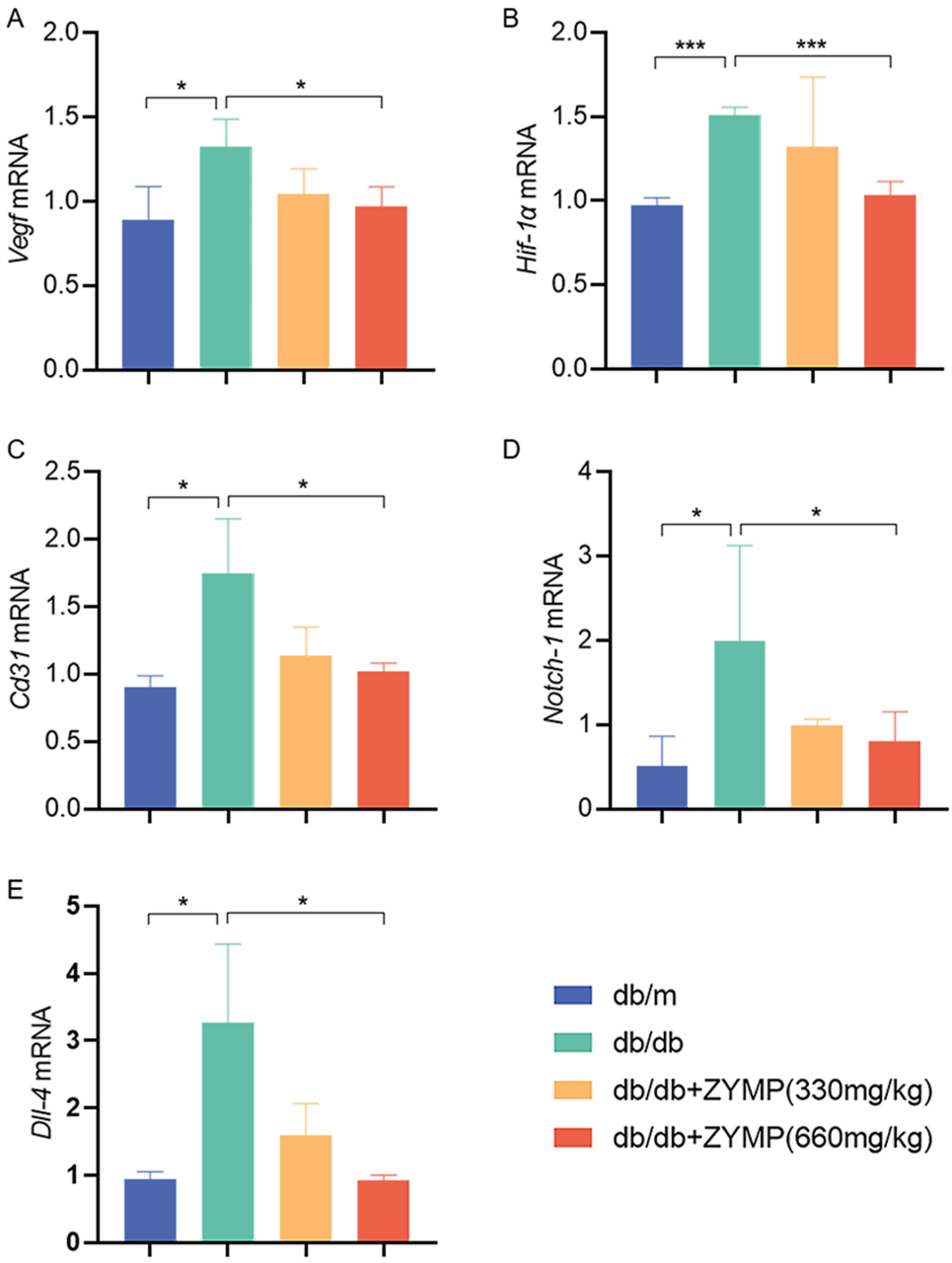

Figure 7 ZYMT inhibits neoangiogenesis in db/db mice. (**A**–**E**). The mRNA levels of *Vegf*, *Hif-1α*, *Cd31*, *Notch-1* and *Dll-4* were determined by RT-qPCR. Data are mean ± SD. **P*<0.05, ****P*<0.001.

A (RELA, namely nuclear factor-kappa B3 (NF-κB3)), belonging to the NF-κB family, plays an important role in the inflammatory response. NF-κB is the main target of hyperglycemia and oxidative stress and can regulate genes related to inflammatory response (tumor necrosis factor-alpha (TNF-α), interleukin-1 beta (IL-1β), and IL-6, etc).[20] The phosphorylation of RELA serine 536 can negatively regulate NF-κB, which results in the regulation of inflammatory response.[21] HIF-1α is a transcription factor that is activated and stabilized in a hypoxic environment and induces the activation of VEGF, which is essential for neovascularization in DR.[22] Increased expression of TNF-α and IL-6 can also cause increased expression of VEGF, which leads to inflammatory response. Massive infiltration of inflammatory cells leads to the destruction of retinal structure and function and ultimately DR. B-cell lymphoma-2 (BCL-2) and BCL2 associated X, apoptosis regulator (BAX) genes in the BCL2 family are the most important genes involved in regulating apoptosis. BCL-2 and BAX not only act as the upstream regulatory mechanism of caspase-3 and participate in the regulation of

https://doi.org/10.2147/DMSO.S495286

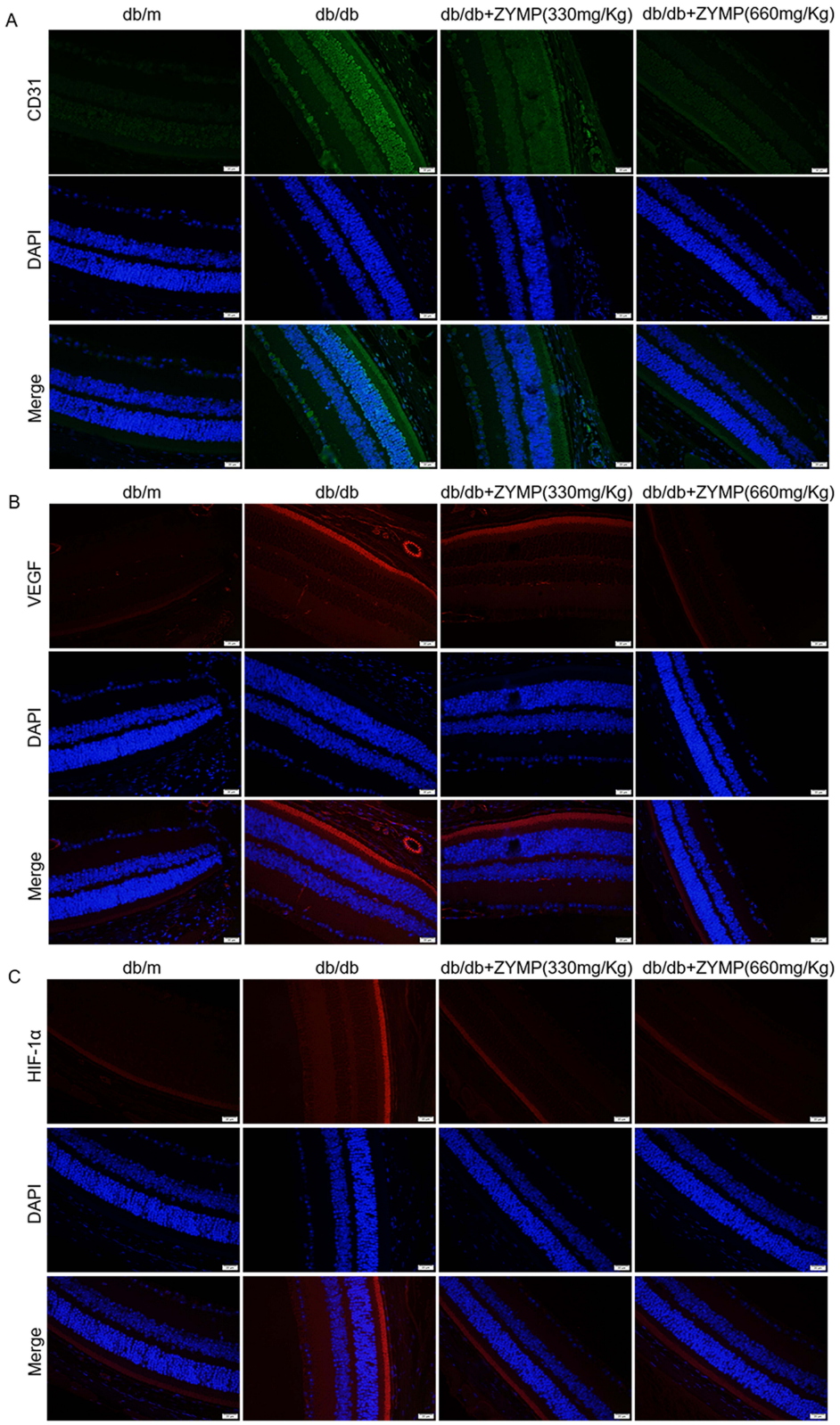

Figure 8 ZYMT inhibits neoangiogenesis in db/db mice. (**A**–**C**). Representative images of immunofluorescence staining of CD31, VEGF and HIF-1α. Scale Bar, 20 μm.

caspase-3 activity but also act as the direct substrate of caspase-3, and are both interrelated and constrained by each other during apoptosis transduction.[23] Overall, network pharmacological analysis suggests that ZYMT ameliorates DR by modulating the PI3K-AKT signaling pathway, inflammatory response, apoptosis, and HIF-1α/VEGF signaling pathway.

In addition, the effect of ZYMT on DR was further validated in vivo using db/db mice as a DR mouse model. It was found that ZYMT did not improve metabolic indices such as body weight, fasting blood glucose, and blood lipids in DR mice, suggesting that ZYMT has a direct effect on DR rather than a secondary improvement of metabolic indices. Tissue staining studies demonstrated that ZYMT improved retinal vascular morphology and delayed retinal thinning in DR mice. The OCTA imaging also showed that ZYMT increased blood flow density in DR mice.

Moreover, the effect of ZYMT on DR cell apoptosis was verified for further mechanistic investigation, and TUNEL staining showed that ZYMT treatment reduced DR cell apoptosis. Meanwhile, ZYMT increased the expression of the anti-apoptotic gene, Bcl-2, and decreased the expression of the pro-apoptotic gene, BAX. The Notch signaling pathway and its ligand, delta-like ligand 4 (Dll4), play an important role in the regulation of neovascularization.[24] The Notch signaling pathway plays a major role in mediating acinar cell outgrowth, which is coordinated with VEGF signaling pathway. Hypoxia is a key trigger for the activation of the Notch-VEGF signaling pathway. The expression of the HIF-1α gene is upregulated in hypoxic environments, promoting the formation of neovascularization,[25] which is an important mechanism in the development of DR. The endothelial marker CD31 is highly expressed in DR.[26] Our data showed that ZYMT treatment reduced the expression of CD31, HIF-1α, and VEGF proteins, as well as *Cd31, Hif-1α, Vegf, Notch*, and *Dll4* genes, in the retinas of DR mice.

Overall, this study firstly analyzed the therapeutic targets of ZYMT for DR using a network pharmacological approach and then reported for the first time the preventive effect of ZYMT on DR using db/db mice as a mouse model of DR. DR mice exhibited pathological alterations in the retina with increased apoptosis and neovascularization, which were abolished by ZYMT. These findings support the effectiveness of ZYMT for the treatment of DR. The current study only explored the effects of ZYMT on DR apoptosis and regulation of HIF-1α/VEGF in vivo; however, whether ZYMT can modulate the PI3K/AKT signaling pathway and inflammation to affect DR warrants further investment.

Conclusion

In summary, the present study combined network pharmacological analysis and in vivo experiments and reports for the first time that ZYMT can improve DR by inhibiting apoptosis and anti-neovascularization, further supporting the use of ZYMT as an effective strategy for the clinical treatment of DR.

Ethics Statement

This study has been approved by the Experimental Animal Ethics Committee of Qilu Hospital of Shandong University (ethics approval number: DWLL-2022-071), complying with the Regulations on the Administration of Experimental Animals of Shandong Province (dated January 24, 2018).

The network pharmacology study involved database relating to human data, including GeneCards, DisGeNET, and Online Mendelian Inheritance in Man (OMIM) database and STRING database. The study is exempt from approval as the data were retrieved from the publicly available data, based on Measures for Ethical Review of Life Science and Medical Research Involving Human Subjects (China, February 18, 2023), according to Item 1 and 2 of Article 32.

Acknowledgments

This study was supported by the Youth Fund of National Natural Science Foundation (grant number 82200918); Youth Fund of Shandong Natural Science Foundation (grant number ZR2021QC111).

Author Contributions

All authors made a significant contribution to the work reported, whether that is in the conception, study design, execution, acquisition of data, analysis and interpretation, or in all these areas; took part in drafting, revising, or critically reviewing the article; gave final approval of the version to be published; have agreed on the journal to which the article has been submitted; and agree to be accountable for all aspects of the work.

Disclosure

Na Ning, Qiuling Huang and Jiajia Hu are employees of Guangzhou Baiyunshan Zhongyi Pharmaceutical Co. Ltd. In addition, they have a pending patent related to the application of Zhangyangming Tablets in alleviating retinitis pigmentosa (license No. WO 2023/168898 A1). The authors declare that they have no other conflicts of interest in this work.

References

1. Saeed M, Shoaib A, Tasleem M, et al. Role of alkannin in the therapeutic targeting of protein-tyrosine phosphatase 1b and aldose reductase in type 2. *Diabetes*. 2024;9(34):36099–36113. doi:10.1021/acsomega.4c00082
2. Wong TY, Cheung CMG, Larsen M, Sharma S, Simó R. Diabetic retinopathy. *Nat Rev Dis Primers*. 2016;2:16012. doi:10.1038/nrdp.2016.12
3. Teo ZL, Tham Y-C, Yu M, et al. Global prevalence of diabetic retinopathy and projection of burden through 2045: systematic review and meta-analysis. *Ophthalmology*. 2021;128(11):1580–1591. doi:10.1016/j.ophtha.2021.04.027
4. Song P, Yu J, Chan KY, Theodoratou E, Rudan I. Prevalence, risk factors and burden of diabetic retinopathy in China: a systematic review and meta-analysis. *J Global Health*. 2018;8(1):010803. doi:10.7189/jogh.08.010803
5. Kollias AN, Ulbig MW. Diabetic retinopathy: early diagnosis and effective treatment. *Deutsches Arzteblatt Int*. 2010;107(5). doi:10.3238/arztebl.2010.0075
6. Liu Y, Wu N. Progress of nanotechnology in diabetic retinopathy treatment. *Int J Nanomed*. 2021;16:1391–1403. doi:10.2147/IJN.S294807
7. Ai X, Yu P, Hou Y, et al. A review of traditional Chinese medicine on treatment of diabetic retinopathy and involved mechanisms. *Biomed Pharmacothe*. 2020;132:110852. doi:10.1016/j.biopha.2020.110852
8. Huang Z, Huang Q, Xu K, et al. Protective effect of ZYMT, a traditional Chinese patent medicine in a mouse model of retinitis pigmentosa. *Biomed Pharmacothe*. 2023;162:114580. doi:10.1016/j.biopha.2023.114580
9. Kang Q, Yang C. Oxidative stress and diabetic retinopathy: molecular mechanisms, pathogenetic role and therapeutic implications. *Redox Biol*. 2020;37:101799. doi:10.1016/j.redox.2020.101799
10. Alshaghdali K, Tasleem M, Rezgui R, et al. Cucumis melo compounds: a new avenue for ALR-2 inhibition in diabetes mellitus. *Heliyon*. 2024;10(15):e35255. doi:10.1016/j.heliyon.2024.e35255
11. Ardourel M, Felgerolle C, Pâris A, et al. Dietary supplement enriched in antioxidants and omega-3 promotes glutamine synthesis in müller cells: a key process against oxidative stress in retina. *Nutrients*. 2021;13(9):3216. doi:10.3390/nu13093216
12. Zhang Q, Yao M, Qi J, et al. Puerarin inhibited oxidative stress and alleviated cerebral ischemia-reperfusion injury through PI3K/Akt/Nrf2 signaling pathway. *Front Pharmacol*. 2023;14:1134380. doi:10.3389/fphar.2023.1134380
13. Song H, Xiong M, Yu C, et al. Huang-Qi-Jian-Zhong-Tang accelerates healing of indomethacin-induced gastric ulceration in rats via anti-inflammatory and antioxidant mechanisms. *J Ethnopharmacol*. 2024;319(Pt 2):117264. doi:10.1016/j.jep.2023.117264
14. Saeed M, Tasleem M, Shoib A, et al. Identification of putative plant-based ALR-2 inhibitors to treat diabetic peripheral neuropathy. *Curr Issues Mol Biol*. 2022;44(7):2825–2841. doi:10.3390/cimb44070194
15. Yang M, Cui Y, Song J, et al. Mesenchymal stem cell-conditioned medium improved mitochondrial function and alleviated inflammation and apoptosis in non-alcoholic fatty liver disease by regulating SIRT1. *Biochem Biophys Res Commun*. 2021;546:74–82. doi:10.1016/j.bbrc.2021.01.098
16. Zhang Z, Liu H, Liu J. Akt activation: a potential strategy to ameliorate insulin resistance. *Diabetes Res Clin Pract*. 2019;156:107092. doi:10.1016/j.diabres.2017.10.004
17. Yu N, Fang X, Zhao D, et al. Anti-Diabetic effects of Jiang Tang xiao ke granule via PI3K/Akt signalling pathway in type 2 diabetes KKAy mice. *PLoS One*. 2017;12(1):e0168980. doi:10.1371/journal.pone.0168980
18. Li J, Chen K, Li X, et al. Mechanistic insights into the alterations and regulation of the AKT signaling pathway in diabetic retinopathy. *Cell Death Discovery*. 2023;9(1):418. doi:10.1038/s41420-023-01717-2
19. Papa S, Choy PM, Bubici C. The ERK and JNK pathways in the regulation of metabolic reprogramming. *Oncogene*. 2019;38(13):2223–2240. doi:10.1038/s41388-018-0582-8
20. Li W, Shen X, Wang Y, Zhang J. The effect of Shengpuhuang-tang on retinal inflammation in streptozotocin-induced diabetic rats by NF-κB pathway. *J Ethnopharmacol*. 2020;247:112275. doi:10.1016/j.jep.2019.112275
21. Zhao Y, Banerjee S, Dey N, et al. Klotho depletion contributes to increased inflammation in kidney of the db/db mouse model of diabetes via RelA (serine)536 phosphorylation. *Diabetes*. 2011;60(7):1907–1916. doi:10.2337/db10-1262
22. Catrina S-B, Zheng X. Hypoxia and hypoxia-inducible factors in diabetes and its complications. *Diabetologia*. 2021;64(4):709–716. doi:10.1007/s00125-021-05380-z
23. Zhao H, Yenari MA, Cheng D, Sapolsky RM, Steinberg GK. Bcl-2 overexpression protects against neuron loss within the ischemic margin following experimental stroke and inhibits cytochrome c translocation and caspase-3 activity. *J Neurochem*. 2003;85(4):1026–1036. doi:10.1046/j.1471-4159.2003.01756.x
24. Bentley K, Franco CA, Philippides A, et al. The role of differential VE-cadherin dynamics in cell rearrangement during angiogenesis. *Nat Cell Biol*. 2014;16(4):309–321. doi:10.1038/ncb2926
25. Ren J-S, Bai W, Ding -J-J, et al. Hypoxia-induced AFAP1L1 regulates pathological neovascularization via the YAP-DLL4-NOTCH axis. *J Transl Med*. 2023;21(1):651. doi:10.1186/s12967-023-04503-x
26. Tian B, Li X-X, Shen L, Zhao M, Yu W-Z. Auto-mobilized adult hematopoietic stem cells advance neovasculature in diabetic retinopathy of mice. *Chin Med J*. 2010;123(16):2265–2268. doi:10.3760/cma.j.issn.0366-6999.2010.16.020

Diabetes, Metabolic Syndrome and Obesity

Dovepress
Taylor & Francis Group

Publish your work in this journal

Diabetes, Metabolic Syndrome and Obesity is an international, peer-reviewed open-access journal committed to the rapid publication of the latest laboratory and clinical findings in the fields of diabetes, metabolic syndrome and obesity research. Original research, review, case reports, hypothesis formation, expert opinion and commentaries are all considered for publication. The manuscript management system is completely online and includes a very quick and fair peer-review system, which is all easy to use. Visit http://www.dovepress.com/testimonials.php to read real quotes from published authors.

Submit your manuscript here: https://www.dovepress.com/diabetes-metabolic-syndrome-and-obesity-journal